0041-1337/01/7109-1249/0
TRANSPLANTATION
Vol. 71, 1249–1256, No. 9, May 15, 2001
Printed in U.S.A.

ORTHOGONAL POLARIZATION SPECTRAL IMAGING AS A TOOL FOR THE ASSESSMENT OF HEPATIC MICROCIRCULATION

A VALIDATION STUDY

STEFAN LANGER,[1,2] ANTHONY G. HARRIS,[3] PETER BIBERTHALER,[1] ERNST VON DOBSCHUETZ,[1] AND KONRAD MESSMER[1]

Institute for Surgical Research, Ludwig-Maximilians-University Munich, University Hospital Grosshadern, 81366 Munich, Germany, and Cytometrics Inc., Philadelphia, Pennsylvania

Background. **Quantitative analysis of liver microcirculation using intravital fluorescence microscopy in animals has increased our knowledge about ischemia-reperfusion injury. However, because of the size of the instrumentation and the necessity of fluochromes for contrast enhancement, human liver microcirculation cannot be observed. Orthogonal Polarization Spectral (OPS) imaging is a recently introduced technique that can be used to visualize the microcirculation without the need for fluorescent dyes. It is a small, hand-held device and could potentially be used to study the microcirculation of the human liver in a clinical setting. However, before implementation into clinical use its ability to quantitatively measure microcirculatory parameters must be validated.**

Methods. **The livers of Spraque-Dawley rats (n=9) were exteriorized, and images were obtained using OPS imaging and intravital fluorescence microscopy of the identical microvascular regions before and after the induction of a 20-min warm lobar ischemia. Images were videotaped for later computer-assisted off-line analysis.**

Results. **OPS imaging can be used to accurately quantify the sinusoidal perfusion rate, vessel diameter, and venular red blood cell velocity. Correlation parameters were significant and Bland-Altman analyses showed good agreement for data obtained from the two methods at baseline as well as during reperfusion.**

Conclusion. **OPS imaging can be used to quantitatively measure microcirculatory parameters in the rat liver under both physiological and pathophysiological conditions. Thus, OPS imaging has the potential to be used to make quantitative measurements of the microcirculation in the human liver.**

Interruption of the blood flow to the liver is frequently applied during liver surgery and unavoidable in organ transplantation. The resulting injury to the tissue is known to be the source of the major perioperative complications (*1–3*). After ischemia, the reestablishment of blood flow and reoxygenation produces the so-called ischemia-reperfusion injury (I/R), which is associated with organ dysfunction and cell death (*4–6*). Using intravital fluorescence microscopy (IFM), combined with fluorescent dyes for contrast enhancement, the effects of I/R on the hepatic microcirculation have been studied extensively in animals by many researchers (*7–10*). Moreover, studies have been performed to investigate the microcirculatory disturbances that occur during hemorrhagic shock as well as liver transplantation (*11–14*). These investigations have comprehensively analyzed the functions of hepatic microcirculation and have provided significant information about the microcirculatory pathophysiology of the liver in animal models.

Similar studies could not be performed in humans because the human liver was not accessible for intravital microscopy. This was due to the large size of the microscopic equipment required and the necessity of fluorescent dyes for contrast enhancement. Since the dyes themselves are toxic and are associated with the danger of phototoxic effects (*15*, *16*), they cannot used in patients.

The ability to asses the microcirculation of the human liver would provide important diagnostic information about the degree of I/R that occurs during surgery and transplantation. Moreover, the quality of perfusion of a potential liver graft could be assessed before its explantation, and tissue perfusion could be monitored after the reestablishment of blood flow at the recipient site. Therefore, a method that allows for routine clinical assessment of hepatic microcirculation in humans would be of great clinical importance.

The recently introduced technique of Orthogonal Polarization Spectral (OPS) imaging could provide a method to study the human liver microcirculation. This technique can be used to obtain images of the microcirculation without the use of fluorescent dyes (*17*). In OPS imaging the contrast is obtained from the absorption of light by the hemoglobin in the blood. Hence, the hemoglobin-carrying structures appear in negative contrast compared with the surrounding tissue. OPS imaging has been incorporated into a small, hand-held, easy-to-use device called the CYTOSCAN A/R (Fig. 1). Before clinical applications can be developed, the technology must first be validated for quantitative microvascular measurements. Therefore, the aim of the present study was to validate OPS imaging against standard IFM under normal and pathophysiological conditions in the rat liver.

MATERIALS AND METHODS

Animals. Nine male Spraque-Dawley rats (220–240 g body weight) were obtained from Charles River Wiga, Sulzfeld, Germany. They were housed in groups of two in a cage at 21C° temperature in a 12 hr dark/12 hr light cycle and had access to ordinary laboratory

[1] Institute for Surgical Research, Ludwig-Maximilians-University Munich, University Hospital Grosshadern.

[2] Address correspondence to: Dr. med. Stefan Langer, Clinic for Plastic and Hand Surgery/Burn Unit, Ruhr University, 44789 Bochum, Germany, email: Stefan.Langer@ruhr-uni-bochum.de

[3] Cytometrics Inc.

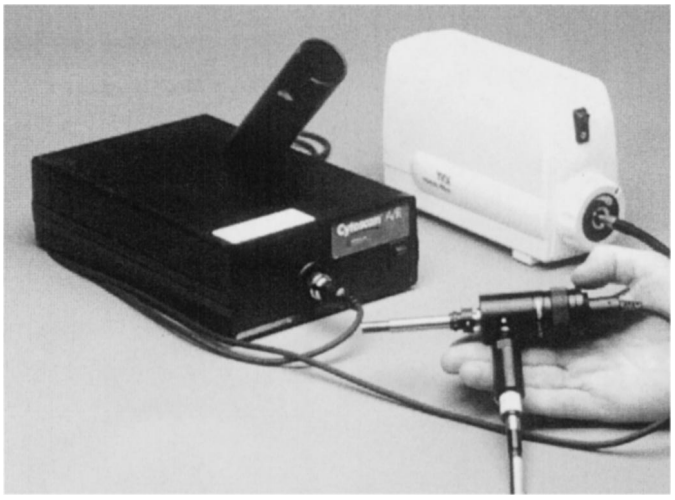

FIGURE 1. The CYTOSCAN A/R instrument. The main parts of the device are the base unit (left) with an holster for the probe on the top of it. The probe (in front) is connected to an external light source (right) via a liquid light guide cable and emits green light of a wavelength of 548 nm during operation. The CCD camera connector cable (at the rear of the probe) is plugged into the base unit. With a standard VCR and monitor, online imaging as well as recording of the images can be performed.

chow (18000 IE/kg vitamin A, 1280 IE/kg vitamin D3, 120 mg/kg vitamin E; sniff, Spezialdiaeten, Soest, Germany) and tap water ad libitum before the experiments. The experimental procedures were performed in accordance with the German legislation on the protection of animals.

Surgical preparation. The model used has been described in detail previously (*9*, *18–20*). Briefly, after overnight fasting with free access to tap water, the animals were anesthetized with an intraperitoneal injection of pentobarbital (50 mg/kg body weight; Rhone Merieux GmbH, Laupheim, Germany) and placed on a heated operating table to maintain body temperature at 37.0°C. The animals were tracheotomized and mechanically ventilated (Effenberger, Munich, Germany). Catheters (inner diameter 0.58 mm; Portex, Hythe, England) were inserted into the right carotid artery and jugular vein for monitoring systemic arterial pressures and blood gases, to continuously infuse Ringer's solution (35 μL/min/100 g body weight), and for the injection of additional pentobarbital.

After a transverse abdominal incision, the ligaments around the liver were dissected to mobilize the left liver lobe. After a waiting period (20 min) to confirm the stability of arterial blood pressure, the left lobe of the liver was exteriorized on an custom-made stage to immobilize it and also to eliminate movements caused by the mechanical ventilation. The lower surface of the liver was placed horizontal to insure that the entire field of view was in focus using OPS imaging and IFM.

After exteriorization, the left liver lobe was covered with a specially designed cover glass (Zeiss, Oberkochen, Germany) that has a sequentially numbered grid with a side length of 300 μm etched into its surface (*21*). The cover slide was immersed with warm (37°C) sterile saline.

Using the computer-controlled XY-stage of the intravital microscopy setup (*22*) the identical sites of interest of the liver surface, which were stored in the computer, could easily be relocated at each time point during the experimental protocol. The numbered grid of the cover glass was used to insure that the identical microvascular regions of interests were located. At the end of the experiment the animal was killed by an overdose of pentobarbital.

Investigations using IFM. The intravital microscope used for the study has been described in detail previously (*22*). After surgical preparation the animal was positioned underneath the optics of the IVM setup. Therefore, the operating stage with the animal on it was placed on the computer-controlled XY-plate of the microscope and locked in place by means of two pins fitting in appropriate pinholes. For microcirculatory studies sodium fluorescein (10^{-6} M/kg per animal; approximately 0.3 ml; Merck, Darmstadt, Germany) was injected via the jugular catheter for contrast enhancement. A filter combination of 450–490 nm/>490 nm (excitation/emission) and a 12-volt, 150 watt halogen light source (Zeiss, Oberkochen, Germany) were used for the visualization of sodium fluorescein. A 20× Zeiss water immersion objective was used for epi-illumination and resulted in a final on-screen magnification of ×533.

The IFM images were captured using a charge-coupled device video camera (FK 6990; Piper, Schwerte, Germany) and recorded on superVHS video tapes (Sony, Cologne, Germany) for later off-line computer-assisted analysis.

Investigations using OPS imaging. To take advantage of the computer-controlled XY-plate, the OPS imaging probe (CYTOSCAN A/R; Cytometrics, Inc., Philadelpia, PA) was attached at the shaft of the IFM setup. To identify the exact same site of interest with the two techniques, the operating stage had two different pairs of pinholes. By switching between the two pairs of holes the identical region of interest could be located either with the OPS imaging probe or the IFM.

The OPS images were captured on the identical videotapes and using the same video recorder as for IFM. The objective of the OPS imaging probe was covered with a disposable sterile plastic lens to protect the OPS imaging probe during operation. The final on-screen magnification of the images obtained with the OPS imaging device was ×450.

Experimental protocol. After a stabilizing period of 20 min, the baseline conditions of the microcirculation were recorded with both OPS imaging and IFM. After that, the livers were subjected to an isolated warm left lobar ischemia for 20 min by clamping the left branch of the hepatoduodenal ligament by means of a surgical microclip (Aesculap, Tuttlingen, Germany). Immediately after clip removal (0 min) as well as at the time points 30, 60, and 120 min after postischemic reperfusion, images of hepatic microcirculation were recorded with OPS imaging and IFM at the identical positions as were recorded at baseline.

Analysis of microcirculation. To investigate alterations of hepatic microcirculation in the individual animal 10 liver acini and 6 postsinusoidal venules were randomly selected and their coordinates stored in the computer. The observation time for each region of interest was limited to 20 sec for each system to prevent phototoxic effects (*15*). The following four parameters were analyzed:

1. The sinusoidal perfusion rate [%], given as the number of perfused sinusoids divided by the number of all observed sinusoids present in the midzonal segment.

2. The diameter of sinusoids of the midzonal segment of each acinus [μm].

3. The diameter of postsinusoidal venules [μm]

4. The midstream red blood cell velocity of postsinusoidal venules [mm/sec]. The sinusoidal perfusion rate was assessed by frame-to-frame observations of the videotaped images. The other parameters were evaluated off-line by using the CapImage computer program (Dr. Zeintl, Heidelberg, Germany) (*23*).

Statistics. The data are presented as mean ± SEM. For analysis of correlation between data obtained from OPS imaging and IFM a linear regression analysis and Spearman rank-order correlation were established. Repeated analysis of variance (ANOVA) followed by the Dunn's method was performed to compare differences between time steps. A P value less than 0.05 was considered as statistically significant.

The data were further analyzed according to the method of Bland and Altman, which is a supplementary method to compare two different methods when the true value is not known (*24*, *25*). The

data are plotted as scatter plots of the mean values of the two methods versus the difference between the two methods. Agreement was evaluated as mean difference (bias) and standard deviation of the difference (precision). Moreover the values that are located inside the 95% confidence interval and the range of this interval are given.

RESULTS

It was possible to perform successive observations of the identical microvascular sites of interest using OPS imaging and IFM at baseline and during postischemic reperfusion. Typical images captured using OPS imaging and standard IFM of the identical site of interest are shown in Figure 2. The morphological structures of the liver microvasculature could be clearly identified using OPS imaging, and it was possible to make accurate quantitative measurements of microcirculatory parameters under both baseline conditions and during reperfusion.

Hepatic microcirculation was affected by a 20-min warm lobar ischemia as can be seen in Figure 3. For the direct comparison of the data obtained with the two techniques, the results are presented in Table 1. To demonstrate that OPS imaging can be used to successfully determine microvascular disturbances, in the following section the results from the OPS imaging device are given. In detail, sinusoidal perfusion rate dropped significantly after the onset of reperfusion to 81.6±2.6% as compared with baseline values (98.4±0.6%) and recovered to 93.2±1.8% at the end of the reperfusion time.

Immediately after the onset of reperfusion, sinusoidal diameter was significantly attenuated and reduced from 10.2±0.1 μm at baseline to 9.5±0.1 μm. By the 30 min time point, the diameter was no longer significantly different, and there was a tendency to regain baseline values (9.9±0.1 μm, 120 min).

In postsinusoidal venules there was an apparent reduction of diameter after ischemia; however, no significant differences were seen.

Venular red blood cell velocity was significantly reduced immediately after the start of reestablishment of blood flow (baseline: 0.61±0.03 mm/sec; 0 min: 0.46±0.02 mm/sec) and was further characterized by a steady complete recovery during the time course in such a way that baseline values were achieved at 120 min of reperfusion (0.61±0.01 mm/sec). Systemic blood pressure remained constant throughout the entire protocol (data not shown).

Comparison between OPS imaging and IFM. As illustrated in Figure 4, regression analysis showed a high correlation between the two methods for sinusoidal perfusion rate (r^2=0.82). Additionally, a combined Bland-Altman plot for the data is shown. The combination of the data into a single plot is justified because the plots for all the time points were very similar. Bias, as analyzed by the Bland-Altman method, was −0.01 with a precision of 0.8. The slope of the linear fit was almost zero (y=0.07x+0.59). Further, the percentages of the total numbers of values located outside the 95% confidence interval was small (5.8%) and the 95% confidence interval was located at ±1.6 so that a strong agreement between the two techniques was observed. In Figures 5–7 the regression analysis and Bland-Altman plots for the other measured microcirculatory parameters are presented. They also demonstrate a good agreement between the two techniques.

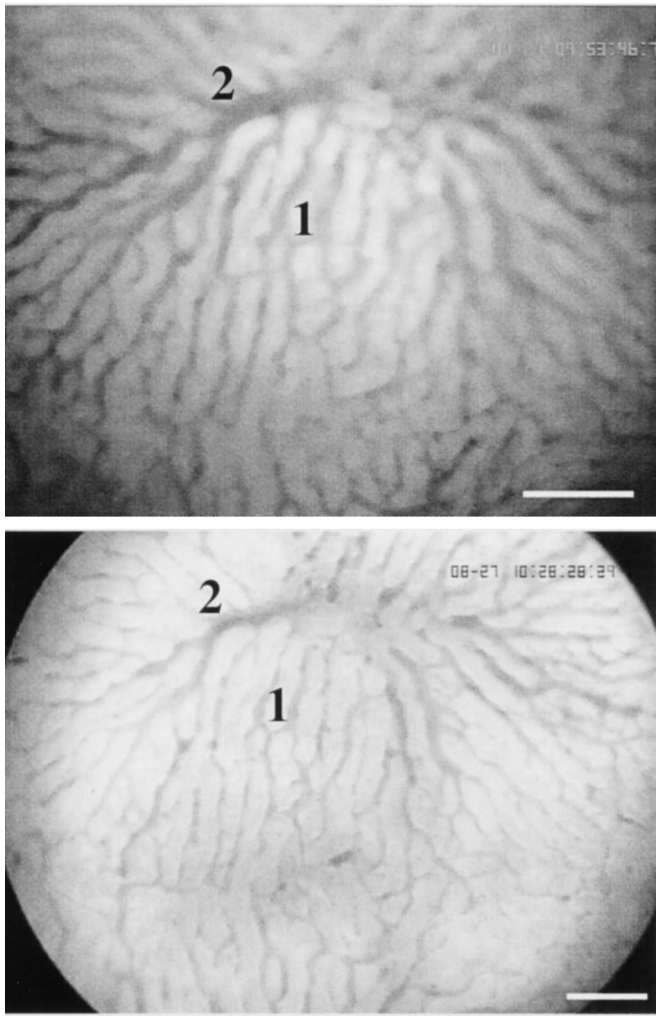

FIGURE 2. (Top) Intravital fluorescent microscopy. The microcirculation of the rat liver surface as recorded with standard IVM is shown. The typical structure of a liver acinus is contrasted by the systemic application of sodium-fluorescein as a fluorescent dye. Since sodium-fluorescein leaks out of the microcirculation, its structure appears in a positive contrast. The images were captured under baseline conditions. (1=indicates liver sinusoids; 2=indicates a postsinusoidal venule). (Bottom) OPS imaging. The identical microvascular area as shown above recorded with the CYTOSCAN A/R instrument. Using OPS imaging the tissue is illuminated with linearly polarized light and imaged through a polarizer oriented orthogonal to the plane of the illuminating light. Since polarization is preserved in reflection only photons scattered relatively deep in the tissue contribute to the images. OPS imaging forms thereby a virtual light source within the tissue, so that vessels appear black as is the case in IVM. However, there is no need for any fluorescent dye. The quality and the contrast of the CYTOSCAN A/R images are comparable to those recorded with standard intravital microscopy. Bar: 100 μm.

Correlation parameters and the Bland-Altman analyses were similar during baseline and reperfusion, indicating that OPS imaging is a reliable technique not only for measurements during physiological states but for use at pathophysiological states when the tissue is injured.

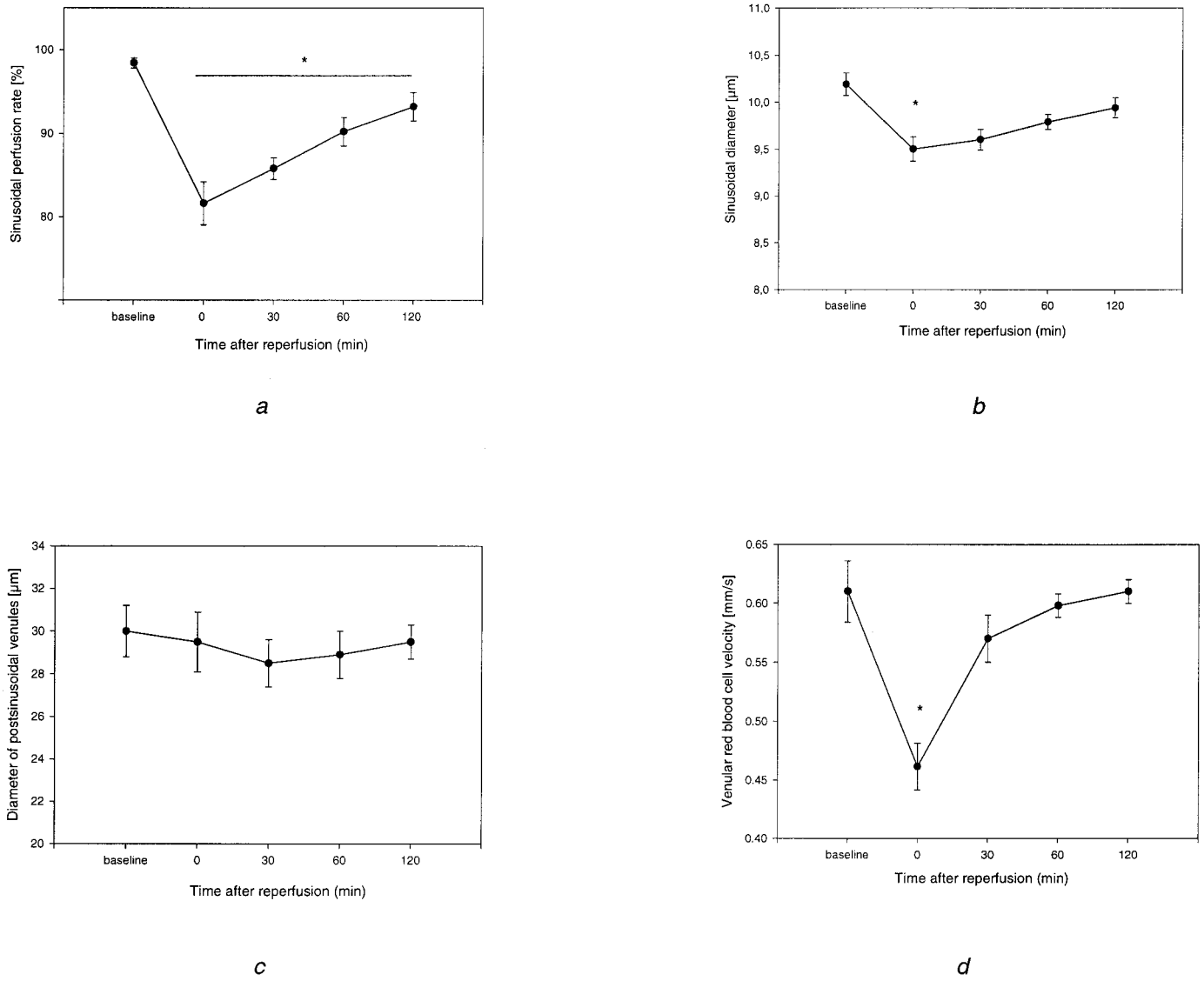

FIGURE 3. Effect of I/R on hepatic microcirculation. Results from OPS imaging analysis. (a) Time course of hepatic sinusoidal perfusion rate is presented. Perfusion rate is given as the percentage of perfused sinusoids versus all observed sinusoids per acinus for baseline and the reperfusion period. During reperfusion there is a significant reduction of perfused sinusoids as compared with baseline. * Indicates $P<0.05$ versus baseline values. Mean ± SEM repeated ANOVA followed by Dunn's method. (b) Changes in sinusoidal diameter from baseline to reperfusion are presented. Sinusoidal diameter is given as the average sinusoidal diameter measured at the midzonal area of the acinus (n=10 per animal). * Indicates $P<0.05$ versus baseline values. Mean ± SEM repeated ANOVA followed by Dunn's method. (c) Diameter of postsinusoidal venules at baseline and at the different time points of postischemic reperfusion are graphed. There was no statistical difference observed in diameter measurements during reperfusion. Mean ± SEM repeated ANOVA followed by Dunn's method. (d) Red blood cell velocity of postsinusoidal venules during hepatic ischemia/reperfusion. Immediately after reperfusion there was a significant reduction of velocity observed, whereas macrohemodynamic parameters were not influenced. * Indicates $P<0.05$ versus baseline values. Mean ± SEM repeated ANOVA followed by Dunn's method.

DISCUSSION

In this methodological article the validation of a new type of intravital microscope, the OPS imaging instrument, was performed. With the OPS imaging technique it was possible to obtain high-quality images of the microcirculation of rat liver without a fluorescent dye. From these images accurate quantitative measurements of the sinusoidal perfusion rate, vessel diameter, and red blood cell velocity in postsinusoidal venules could be made.

In the present study we have demonstrated that 20 min of left lobar ischemia was associated with a statistically significant decrease in the perfusion of individual acini during reperfusion. These results are in agreement with previous examinations (*19*). In a previous study, using a model of total hepatic ischemia, more extensive alterations of the microcirculation were observed compared with our study (*9*). Besides a fall of sinusoidal perfusion rate, after a total hepatic ischemia of 20 min, Kondo and coworkers (*9*) observed a

TABLE 1.

Parameter	Time	IFM	OPS imaging
Diameter postsinusoidal venules [μm]	Baseline	30.9±1.2	30.0±1.2
	0 min	30.0±1.3	29.5±1.4
	30 min	29.6±1.2	28.5±1.1
	60 min	29.9±1.0	28.9±1.1
	120 min	29.0±0.9	29.5±0.8
Diameter sinusoids (midzonal) [μm]	Baseline	10.5±0.16	10.2±0.12
	0 min	9.9±0.12[a]	9.5±0.13[a]
	30 min	10.1±0.09	9.6±0.11
	60 min	10.2±0.09	9.7±0.08
	120 min	10.5±0.10	9.9±0.16
Sinusoidal perfusion rate (midzonal) [%]	Baseline	99.5±0.74	98.4±1.8
	0 min	83.9±7.08[a]	81.6±7.73[a]
	30 min	88.8±5.57[a]	85.8±3.91[a]
	60 min	89.0±6.90[a]	90.2±5.02[a]
	120 min	93.3±5.87[a]	93.2±5.07[a]
Venular red blood cell velocity [mm/sec]	Baseline	0.61±0.03	0.61±0.03
	0 min	0.45±0.02[a]	0.46±0.02[a]
	30 min	0.58±0.02	0.58±0.02
	60 min	0.59±0.02	0.60±0.02
	120 min	0.62±0.02	0.61±0.02

Microcirculatory parameters obtained from OPS imaging and IFM for direct comparison of the data. Data are expressed as mean±SEM.
[a] $P<0.05$ vs. baseline, repeated ANOVA.

significantly reduced mean internal diameter of sinusoids and venules, respectively. In our study alterations of vessel diameter have also been demonstrated, however, the

FIGURE 4. (Top) The regression analysis of measurements of hepatic sinusoidal perfusion rate obtained from IFM plotted of the x axis and those from OPS imaging on the y axis. Note that not all of the n=304 values can be identified, because the data points coincide, and are therefore hidden behind each other. The slope of the regression line, which is almost 1, indicates a strong agreement of the data. Further, a significant correlation was calculated in the Spearman rank order. (Bottom) A Bland-Altman plot of the number of perfused sinusoids in the midzonal area of the acini is shown for baseline and postischemic measurements (n=304). For the Bland-Altman analysis the average of the values (x axis) is plotted against the difference (y axis). The solid line represents the mean difference, the dashed lines the 2 standard deviations of the mean difference (95% confidence interval). The dotted line represents a linear fit of the plotted data, which is almost zero. As is the case in the regression analysis, again many of the individual values coincide so that the total number of the values cannot be seen graphically. Almost all of the data points lie within the confidence interval indicating a strong agreement of the two methods. Further, there is no bias in the measurements and the 95% confidence interval is of an acceptable range.

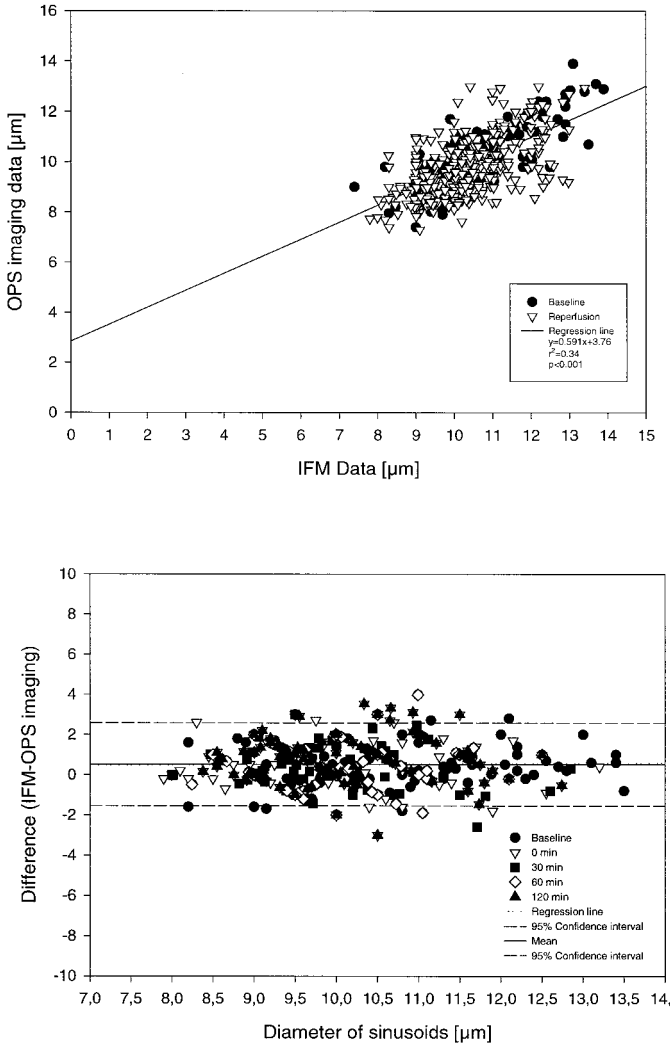

FIGURE 5. (Top) Regression analysis of the measurements of diameter of hepatic sinusoids using OPS imaging and IFM is given. The regression line shows a slope of almost 0.6 for baseline and reperfusion data. There is a statistically significant agreement in the Spearman rank order. (Bottom) The Bland-Altman plot of the measurements of sinusoidal diameter shows 6.4% values out of the 95% confidence interval, which ranges from 2.35 to −1.37. The bias is small (0.49 µm) and the slope of the linear fit is zero. The plot indicates that there is a strong agreement between the data obtained from the two methods.

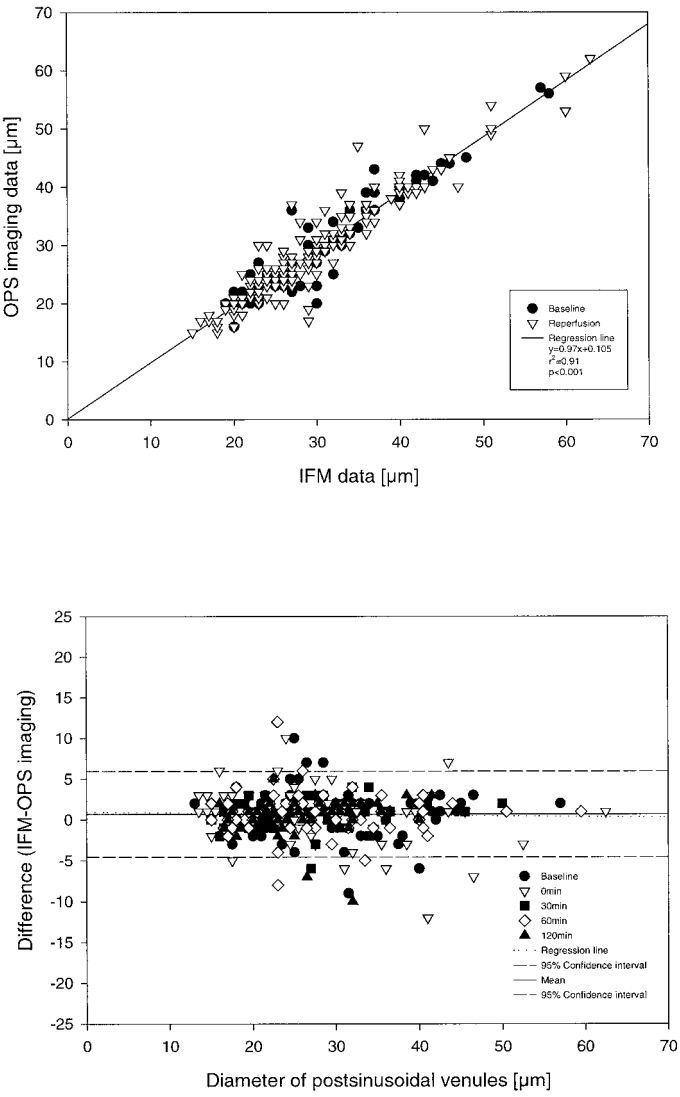

FIGURE 6. (Top) The regression analysis of the measurements of postsinusoidal diameter shows the slope close to 1 (y=0.97x+0.11). The data accumulate all very closely around the linear fit, indicating an excellent correlation of the data obtained with the two methods. Further, in the Spearman rank order there is a significant *P* value. (Bottom) The Bland-Altman plot of the diameter of the postsinusoidal venules of rat liver for all five time points is shown (n=331). The solid line represents the mean difference, which is 0.67 µM. The dashed lines illustrates the 2 standard deviations of the mean difference (95% confidence interval). The linear fit of the plotted data (dotted line) is almost zero, and almost all data points lie within the confidence interval, indicating a excellent correlation of the data.

decrease in venule diameter was not statistically significant as was shown by Kondo et al. (*9*) for both types of vessels.

The reason for the discrepancy in attenuation of vessels diameter and sinusoidal perfusion rate of the two investigations is likely due to the different models of ischemia used. Total hepatic ischemia, as performed in the investigation of Kondo and coworkers (*9*), is known to be accompanied with intestinal congestion, which consequently contributes to liver dysfunction in rats (*26*).

OPS imaging for monitoring hepatic microcirculation. The results of this study show that the OPS imaging technology can be used for the visualization of hepatic microcirculation during physiological and pathophysiological conditions in the rat liver. As can be seen from the correlation parameters, there is a statistically significant agreement of the data obtained from OPS imaging and the standard method for such measurements, the intravital fluorescent microscope. In contrast to the fluorescent method, OPS imaging can be used to visualize the microcirculation in humans because it does not require fluorescent dyes for contrast enhancement (*17*). Furthermore, the OPS imaging device is small and can easily be used in a clinical setting, e.g., during surgery. OPS imaging,

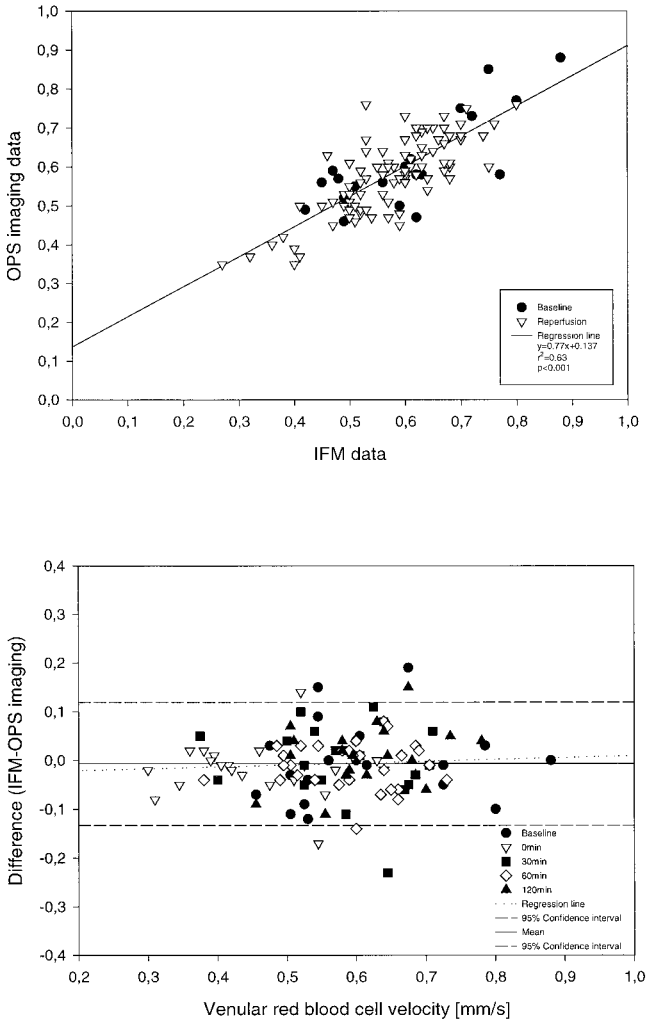

FIGURE 7. (Top) Regression analysis of the measurement of red blood cell velocity in postsinusoidal venules is shown. Regression analysis therefore demonstrates a significant correlation of the values obtained from intravital microscopy and OPS imaging. (Bottom) The Bland-Altman plot of the data demonstrates that there is no bias in the measurements and that the slope of the linear fit is almost zero. Comparison of the results of the measurements of red blood cell velocity using OPS imaging and IFM shows a very strong agreement.

however, does not allow quantification of leukocytes or platelets, as does IFM (*14*, *27*). Therefore, this new technique cannot replace video fluorescent microscopy.

One of the most frequent complications after liver transplantation is the dysfunction of the graft that results from severe deterioration of hepatic microcirculation (*28*). Therefore, the ability to assess blood flow in the human liver is of great clinical importance. Many different techniques have been investigated for their ability to measure blood flow (*29*). Recently, the laser doppler method was used in several investigations to predict liver graft blood flow to identify a compromised microcirculation during transplantation (*30*, *31*) as well as during other surgical procedures (*32*). The major drawback of using the doppler technique, however, is that only relative changes in the blood flow can be measured so that an absolute flow cannot be measured. Further there are a number of factors that make the interpretation of the doppler signal difficult (*33*). Because of this the doppler technique has not found widespread acceptance among clinicians so far.

In contrast, OPS imaging allows for a direct visualization of the microcirculation at the surface of different tissues (*17*), and from these images the computer-assisted quantification of standard microcirculatory parameters (perfusion rate, red blood cell velocity, vessel diameter) is possible. Therefore this technique is advantageous compared with the doppler technique. The ability to monitor microvascular perfusion of the human liver would be of great value in all kinds of procedures necessitating the interruption of the organs' blood supply. From measurements of vessel diameter, red blood cell velocity, and the number of perfused sinusoids, the surgeon could intraoperatively determine the quality of tissue perfusion. I/R could be identified immediately during surgery, which would allow for rapid decision making, e.g., surgical or alternative therapeutic interventions.

Given the success of this validation study on the rat liver, further investigations must now follow to demonstrate that OPS imaging can also successfully be used in humans. Implementation of this novel technique in humans will improve our knowledge of the functions of the microcirculation of the human liver during surgery and transplantation.

Acknowledgments. The authors thank Cytometrics Inc. for making the CYTOSCAN A/R instrument available to our institute. We are grateful to Dr. H. Terajima from Kyoto University for his helpful introduction to the surgical procedure. We also thank Dr. G. Fletcher and Dr. A. Loeb for their help in the preparation of the manuscript.

REFERENCES

1. Delva E, Camus Y, Nordlinger B, et al. Vascular occlusions for liver resections. Operative management and tolerance to hepatic ischemia: 142 cases. Ann Surg 1989; 209; 211.
2. Ploeg RJ, D'Alessandro AM, Knechtle SJ, et al. Risk factors for primary dysfunction after liver transplantation: a multivariate analysis. Transplantation 1993; 55: 807.
3. Huguet C, Gavelli A, Chieco PA, et al. Liver ischemia for hepatic resection: where is the limit? Surgery 1992; 111: 251.
4. Menger MD, Richter S, Yamauchi J, Vollmar B. Role of microcirculation in hepatic ischemia/reperfusion injury. Hepatogastroenterology 1999; 46 (Suppl 2): 1452.
5. Clemens MG, Bauer M, Pannen BH, Bauer I, Zhang JX. Remodeling of hepatic microvascular responsiveness after ischemia/reperfusion. Shock 1997; 8: 80.
6. Massberg S, Messmer K. The nature of ischemia/reperfusion injury. Transplant Proc 1998; 30: 4217.
7. Clemens MG, McDonagh PF, Chaudry IH, Baue AE. Hepatic microcirculatory failure after ischemia and reperfusion: improvement with ATP-$MgCl_2$ treatment. Am J Physiol 1985; 248: H804.
8. Vollmar B, Menger MD, Glasz J, Leiderer R, Messmer K. Impact of leukocyte-endothelial cell interaction in hepatic ischemia-reperfusion injury. Am J Physiol 1994; 267: G786.
9. Kondo T, Todoroki T, Hirano T, Schildberg FW, Messmer K. Impact of ischemia-reperfusion injury on dimensional changes of hepatic microvessels. Res Exp Med (Berl) 1998; 198: 63.
10. Vollmar B, Glasz J, Post S, Menger MD. Role of microcirculatory derangements in manifestation of portal triad cross-clamping-induced hepatic reperfusion injury. J Surg Res 1996; 60: 49.
11. Corso CO, Okamoto S, Rüttinger D, Messmer K. Hypertonic saline dextran attenuates leukocyte accumulation in the liver after hemorrhagic shock and resuscitation. J Trauma 1999; 46: 417.
12. Vollmar B, Lang G, Menger MD, Messmer K. Hypertonic hydroxyethyl starch restores hepatic microvascular perfusion in hemorrhagic shock. Am J Physiol 1994; 266: H1927.
13. Post S, Palma P, Rentsch M, Gonzalez AP, Menger MD. Differential

impact of Carolina rinse and University of Wisconsin solutions on microcirculation, leukocyte adhesion, Kupffer cell activity and biliary excretion after liver transplantation. Hepatology 1993; 18: 1490.
14. Post S, Menger MD, Rentsch M, Gonzalez AP, Herfarth C, Messmer K. The impact of arterialization on hepatic microcirculation and leukocyte accumulation after liver transplantation in the rat. Transplantation 1992; 54: 789.
15. Saetzler RK, Jallo J, Lehr HA, et al. Intravital fluorescence microscopy: impact of light-induced phototoxicity on adhesion of fluorescently labeled leukocytes. J Histochem Cytochem 1997; 45: 505.
16. Steinbauer M, Harris AG, Abels C, Messmer K. Initiation and prevention of phototoxic effects in intravital fluorescence microscopy in the hamster dorsal skinfold chamber. Langenbecks Arch Surg 2000; 385: 290.
17. Groner W, Winkelman JW, Harris AG, et al. Orthogonal polarization spectral imaging: a new method for study of the microcirculation. Nat Med 1999; 5: 1209.
18. Menger MD, Marzi I, Messmer K. In vivo fluorescence microscopy for quantitative analysis of the hepatic microcirculation in hamsters and rats. Eur Surg Res 1991; 23: 158.
19. Vollmar B, Glasz J, Leiderer R, Post S, Menger MD. Hepatic microcirculatory perfusion failure is a determinant of liver dysfunction in warm ischemia-reperfusion. Am J Pathol 1994; 145: 1421.
20. Terajima H, Kondo T, Enders G, et al. Reduction of hepatic microcirculatory failure caused by normothermic ischemia/reperfusion-induced injury by means of heat shock preconditioning. Shock 1999; 12: 329.
21. Kondo T, Okamoto S, Todoroki T, Hirano T, Schildberg FW, Messmer K. Application of a novel method for subsequent evaluation of sinusoids and postsinusoidal venules after ischemia-reperfusion injury of rat liver. Eur Surg Res 1998; 30: 252.
22. Harris AG, Hecht R, Peer F, Nolte D, Messmer K. An improved intravital microscopy system. Int J Microcirc Clin Exp 1997; 17: 322.
23. Klyscz T, Jünger M, Jung F, Zeintl H. [Cap image—a new kind of computer-assisted video image analysis system for dynamic capillary microscopy]. Biomed Tech (Berl) 1997; 42: 168.
24. Bland JM, Altman DG. Statistical methods for assessing agreement between two methods of clinical measurement. Lancet 1986; i: 307.
25. Bland JM, Altman DG. Comparing methods of measurement: why plotting difference against standard method is misleading. Lancet 1995; 346: 1085.
26. Horie Y, Wolf R, Miyasaka M, Anderson DC, Granger DN. Leukocyte adhesion and hepatic microvascular responses to intestinal ischemia/reperfusion in rats. Gastroenterology 1996; 111: 666.
27. Massberg S, Enders G, Leiderer R, et al. Platelet-endothelial cell interactions during ischemia/reperfusion: the role of P-selectin. Blood 1998; 92: 507.
28. Tredger JM. Ischaemia-reperfusion injury of the liver: treatment in theory and in practice. Biofactors 1998; 8: 161.
29. Klar E, Kraus T, Bredt M, et al. First clinical realization of continuous monitoring of liver microcirculation after transplantation by thermodiffusion. Transpl Int 1996; 9 (Suppl 1): S140.
30. Seifalian AM, Chidambaram V, Rolles K, Davidson BR. In vivo demonstration of impaired microcirculation in steatotic human liver grafts. Liver Transpl Surg 1998; 4: 71.
31. Seifalian AM, Mallet SV, Rolles K, Davidson BR. Hepatic microcirculation during human orthotopic liver transplantation. Br J Surg 1997; 84: 1391.
32. Schilling MK, Redaelli C, Krähenbühl L, Signer C, Büchler MW. Splanchnic microcirculatory changes during CO_2 laparoscopy. J Am Coll Surg 1997; 184: 378.
33. Obeid AN, Barnett NJ, Dougherty G, Ward G. A critical review of laser Doppler flowmetry. J Med Eng Technol 1990; 14: 178.

Received 30 May 2000.
Accepted: 22 August 2000.